Surface Activity Profiling of Drugs Applied to the Prediction of Blood−Brain Barrier Permeability

Pekka Suomalainen,[†] Christoffer Johans,*[,†] Tim Söderlund,[‡] and Paavo K. J. Kinnunen[‡]

Kibron Inc., P.O. Box 141, FIN-00171 Helsinki, Finland, and Helsinki Biophysics and Biomembrane Group, Institute of Biomedicine, University of Helsinki, Helsinki, Finland

Received May 19, 2003

The present study describes a novel in vitro platform for physicochemical profiling of compounds, based on their impact on the air/water interfacial tension. Interfacial partitioning coefficient, cross-sectional area, and critical micelle concentration were derived from the Gibbs adsorption isotherms recorded for 76 structurally diverse drugs. An approximation for the membrane partitioning coefficient, K_{memb}, is introduced and calculated for the measured compounds. This methodology provides a fully automatic, high-throughput screening technique for compound characterization, yielding precise thermodynamic information on the partitioning behavior of molecules at air/water interfaces, which can be directly related to their anisotropic interaction with lipid bilayers in biological membranes. The latter represents the barrier for the passive entry of compounds into cells. The surface activity profiles are shown to correlate to the ability of the compounds to pass passively through the blood−brain barrier.

1. Introduction

Because of the large number of drug candidates produced by combinatorial chemistry laboratories, the prediction of ADME (absorption, distribution, metabolism, and excretion) properties has emerged as an issue of primary interest already in the early stages of drug discovery processes. Failure of bringing a drug to the market because of the poor pharmacokinetics/bioavailabilty constitute a large fraction of the total development costs, and thus, the availability of primary screens to distinguish improper compounds has evolved as a central issue. To this end, the ability of compounds to enter into the central nervous system (CNS) from the blood stream is one of the key properties when enhancing the desired beneficial effects of drugs while attenuating their adverse effects. More specifically, in vitro screening for blood−brain barrier (BBB) permeability is of particular importance when developing drugs targeted to CNS disorders, such as Alzheimer disease and psychiatric disorders. Likewise, an unwanted entry into the CNS of drugs aimed at peripheral tissues can result in highly nondesirable side effects. Additionally, knowledge of possible BBB permeation is also important in the development of safe herbicides and pesticides.

The decisive factor for whether a compound can gain access to the brain by passive diffusion is represented by the membranes of the brain capillary endothelial cells and the tight junctions between them. Various approaches to assess drug permeation have been presented, including assays using cultured Caco-2 cell monolayers[1] and artificial membranes (PAMPA).[2] Cell cultures are, however, expensive and seem to suffer from poor reproducibility between different laboratories.[3] The latter approach measures drug permeation through phospholipid impregnated membranes, providing a chemical environment that mimics in vivo cell membrane structures. PAMPA has found extensive use in the prediction of drug absorption, while studies evaluating its benefits in the prediction of BBB permeability are still limited.[4] In addition to the above techniques, physicochemical profiling is used, including measurement of the octanol−water partitioning coefficient (log *P*), as well as calculation of parameters such as polar surface area,[5] hydrogen-bonding descriptors,[6] and filter rules, like Lipinski's rule of five.[7] All these methods have certain advantages but nevertheless sometime fail to provide reliable estimates of the BBB properties of compounds. The parameter log *P*, for instance, which is perhaps the most frequently exploited property in structure−activity relationships, can at its best yield parabolic or bilinear relationships.[8] This is easy to understand because a simple isotropic model for membrane partitioning, assessing the ratio of the drug concentrations in water and octanol as respective bulk phases, is inadequate for describing the anisotropic molecular interactions that prevail in the membrane interface, constituted by amphiphilic lipids.[9]

Interestingly, it has been demonstrated that surface activity and amphiphilicity of compounds correlate to several in vivo processes, including blood−brain barrier permeation,[10,11] gastrointestinal absorption,[12] avidity as P-glycoprotein substrate,[13] and development of phospholipidosis.[14,15] There is also evidence showing a correlation of surface activity of compounds to their toxic effects on cells.[16] More specifically, Seelig and coworkers[10,11] used three parameters to characterize the adsorption behavior at the air/water interface: the onset of surface activity, the area of a molecule at the air/water interface, and the critical micelle concentration (cmc). However, the method of surface activity measurement used in these studies was cumbersome, slow, and required rather large amounts of the compounds.

* To whom correspondence should be addressed. Phone: +358 50 341 5559. Fax: +358 9 6811 9229. E-mail: christoffer@kibron.com.
[†] Kibron Inc.
[‡] University of Helsinki.

10.1021/jm0309001 CCC: $27.50
Published on Web 03/02/2004

In this communication, we present a novel approach, which is based on the use of a multichannel microtensiometer and 96-well plates of standard footprint dimensions. Importantly, the required sample volumes are small and the measurement itself is very fast. Further, an equation for the approximation of membrane partitioning is developed and is shown to correlate with blood−brain barrier permeability.

2. Results and Discussion

Surface activity profiles (SAP) for 161 diverse drug compounds were initially measured. Compounds increasing the surface pressure by less than 3 mN/m at 10 mM concentration were excluded from further analysis because this surface pressure increment did not allow the surface activity parameters to be unambiguously defined (69 compounds). Compounds causing surface pressure increase below 3 mN/m were excluded because there was a strong correlation between the calculated cross-sectional area and the maximum surface pressure measured. Accordingly, the cross-sectional areas obtained at pressures below 3 mN/m are larger than those defined by the actual sizes of the respective molecules. The lack of surface activity, reflecting a high solvation energy was not, however, a criteria for classifying compounds as CNS negative or positive (22 CNS− and 26 CNS+, with no in vivo data found for 21 compounds). Yet it must be noted that many of these compounds excluded from the current analysis would be surface active at higher concentrations.

The blood−brain permeation data for the remaining 76 therapeutic compounds were collected from literature sources.[17,18,11] At this stage, 16 of the 92 compounds increasing surface pressure above the 3 mN/m limit had to be excluded because in vivo CNS data were not found. The remaining compounds were classified as those entering the brain (CNS+, $n = 41$) and those that are free of CNS side effects at the therapeutical dose (CNS−, $n = 35$). The surface activity parameters for the compounds with known in vivo properties are compiled in Table 1. In addition, the molecular weights (MW), polar surface areas (PSA), and data on passive in vivo permeation into the central nervous system (CNS±) are listed. Also indicated are compounds that are known to be P-glycoprotein substrates.[19] PSA values were determined as described by Ertl et al.[20] based on fragment contributions using Joelib.[21] On the basis of the above physicochemical descriptors, PSA, MW, and the measured surface activity, the final drug data set appears to be diverse and evenly distributed between CNS positive and CNS negative.

Entry of compounds into the CNS can occur by active transport or passive diffusion. The BBB is characterized by tight intercellular junctions, and accordingly, the solutes must pass through the epithelial cells constituting the BBB. In these cells the rate-determining barrier is constituted by the surrounding phospholipid bilayer membrane. Parameters such as log P,[22] PSA,[5] and solvation energy[23] have been used to estimate the ability of a molecule to cross lipid bilayers. Although these parameters are conceptually similar, the membrane partitioning coefficient can be expected to provide a more realistic measure because it accounts for the highly anisotropic environment prevailing in a bilayer.

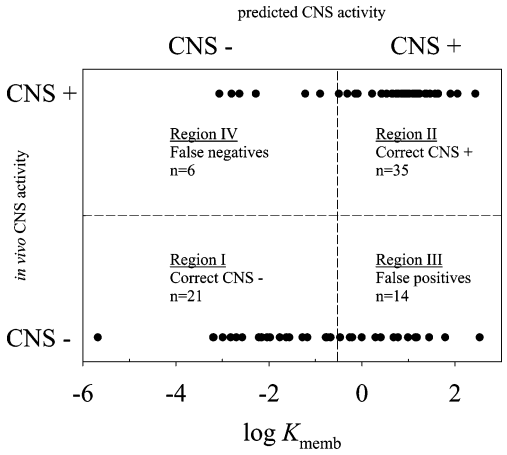

Figure 1. BBB permeability as a function of log K_{memb}.

More specifically, for a compound to cross the BBB it must have not only proper hydrophobicity but also suitable size, shape (conformational flexibility), and distribution of hydrophilic and hydrophobic moieties. All these properties are combined in the membrane partitioning coefficient.

Figure 1 shows the in vivo permeability data as a function of log K_{memb}. Four distinct regions can be observed as follows: (I) CNS− compounds that penetrate the membranes poorly; (II) CNS+ compounds that have large K_{memb}; (III) CNS− compounds that would be expected to enter the brain based on their K_{memb} (false positives); (IV) CNS+ compounds that are predicted not to pass through the BBB (false negatives). When the separating barrier between CNS+ and CNS− was set to a value of −0.5, a maximal predictive score was obtained, with three out of four compounds being correctly classified by log K_{memb}. Because the number of CNS+ compounds was almost equal to the number of CNS− compounds, we consider this to be a good result, especially when taking into account that compounds in region III may involve actively transported substrates as well as those that pass BBB but not do not exhibit receptor binding in the brain and thus lack biological activity in this organ. Additionally, Seelig et al.[13] have shown that membrane partitioning is rate-determining for P-glycoprotein substrates. Such substrates are expected to be false positive (region III); however, some Pgp substrates are found in other regions as well. Nevertheless, in this study 11 out of 16 known Pgp substrates were found above the −0.5 cutoff, suggesting that K_{memb} may be useful in defining the physicochemical characteristics of such substrates. Indeed, it has been argued that amphiphilicity is the only common feature to identify drugs transported by P-glycoprotein.[24]

Figure 2 compares log K_{memb} to a commonly used hydrogen-bonding descriptor, polar surface area (PSA). The two vertical dotted lines shows the upper thresholds reported by Kelder et al.[25] (PSA < 60−70 Å^2) and van de Waterbeemd et al.[17] (PSA < 90 Å^2) for brain penetration. These limits give 67% correct (67% [$n = 30$] above and 67% [$n = 46$] below 65 Å^2) and 68% correct (82 [$n = 17$] above and 59% [$n = 59$] below 90 Å^2) for the compounds investigated in this study for the models by Kelder et al. and van de Waterbeemd et al., respectively. These models seem better for predicting a cutoff PSA

Table 1. Surface Activity Profiling Data[a]

compd	MW [g/mol]	PSA [Å^2]	A_S [Å^2]	cmc [mM]	$\Delta\pi$ [mN/m]	K_{AW} [M^{-1}]	log K_{memb}	Pgp
			Region of CNS−					
acebutolol	336	87.7	160	>10.0	5.6	679	−2.7	
azlocillin	462	173.5	154	>10.0	3.3	202	−3.0	
cloxacillin	436	138.0	136	>10.0	5.0	286	−2.2	
colchicine	399	83.1	168	>10.0	4.1	400	−3.2	x
diclofenac	318	52.2	173	4.4	3.4	570	−3.2	
dicloxacillin	470	138.0	100	>10.0	8.7	612	−0.7	
digoxin	781	203.1	291	0.8	4.3	23134	−5.7	x
disopyramide	340	59.2	129	>10.0	3.8	195	−2.2	
emetine	481	52.2	160	9.5	6.1	866	−2.6	x
enalapril maleate	377	170.5	110	>10.0	7.1	423	−1.2	
fluriprofen	244	37.3	88	>10.0	7.0	236	−0.7	
hydrocortisone	363	94.8	121	>10.0	7.7	771	−1.3	x
ibratrobiumbromide	412	49.8	137	9.7	5.1	369	−2.2	
ketoprofen	254	54.4	111	>10.0	4.1	162	−1.6	
lincomycin	407	147.8	140	>10.0	8.1	1104	−1.8	
methylprednisolone	497	94.8	129	8.7	12.1	4812	−0.8	
metoprolol	267	50.7	126	>10.0	6.5	598	−1.6	
nadolol	309	82.0	118	>10.0	3.1	105	−2.0	
nafcillin	415	121.2	85	>10.0	5.2	156	−0.8	
phenylbutazone	308	40.6	146	>10.0	7.2	1104	−2.0	
timolol	216	108.0	152	>10.0	3.7	263	−2.8	
			Region of CNS+					
alprenolol	286	41.5	106	>10.0	12.8	2425	−0.3	
amitriptyline	277	3.24	60	4.2	19.5	3527	1.5	
apomorphine	267	43.7	48.1	5.0	12.2	567	1.1	
bupropion	240	29.1	66	>10.0	16.1	1077	0.7	
busipirone	386	69.6	125	>10.0	14.4	6623	−0.5	
clomipramine	315	6.5	45	1.3	17.3	3954	2.1	
desipramine	266	15.3	83	>10.0	20.1	5394	0.9	
dextrometorphan	271	12.5	69	>10.0	12.3	656	0.4	
diazepam	285	32.7	70	2.1	10.7	1826	0.8	
diphenylhydramine	225	12.5	68	>10.0	14.7	960	0.6	
doxepin	279	12.5	56	>10.0	20.4	1182	1.1	
flutamide	276	72.2	70	2.3	14.5	4139	1.2	
hydroxyzine	448	35.9	78	3.9	20.7	12243	1.4	
ibuprofen	206	37.3	52	>10.0	13.9	380	0.8	
imipramine	289	6.5	64	>10.0	21.7	2167	1.1	
lidocaine	234	32.3	87	>10.0	10.6	752	−0.1	
maprotilline	277	12.0	58	9.5	20.8	1746	1.2	
mexiletine	179	35.3	76	>10.0	6.7	209	−0.3	
mianserin	264	6.5	84	1.6	13.7	8435	1.0	
nalbuphine	357	73.2	65	>10.0	11.9	461	0.4	
nifedipine	346	107.8	103	1.2	6.5	2992	−0.1	x
nimodipine	419	117.0	60	0.2	15.3	31029	2.4	
nortriptylline	263	12.0	75	5.9	18.1	4176	1.0	
orphenadrine	269	12.5	87	9.6	15.7	2610	0.4	
perphenazine	404	55.3	75	0.6	13.6	17299	1.6	x
progesterone	315	34.1	103	0.5	9.7	15695	0.7	x
promazine	284	31.8	55	4.5	20.4	2869	1.6	
propranolol	259	41.5	66	9.7	15.9	1163	0.8	
protriptyline	263	12.0	72	>10.0	19.3	2724	1.0	
pyrilamine	285	25.4	92	>10.0	11.6	1099	−0.1	
tetracaine	264	41.6	62	>10.0	24.0	3195	1.4	
thioridazin	371	57.1	56	0.5	11.9	6680	1.9	x
tradazone	368	35.9	64	2.7	13.1	2284	1.2	
urapidil	388	71.7	59	>10.0	8.0	175	0.2	
verapamil	455	64.0	93	2.5	15.9	13030	0.9	x
yohimbine	354	65.6	60	9.5	11.7	386	0.5	x
			Region of False Positives					
astemizole	459	42.3	107	0.3	12.0	67270	1.1	
chlorambucil	304	40.5	60	9.8	18.0	1164	1.0	
cyclophosphamide	261	51.4	141	>10.0	3.3	173	−2.6	
daunorubicin	528	185.8	70	0.5	10.1	7190	1.4	x
diflunisal	250	57.5	76	>10.0	9.2	416	0.0	
domperidone	426	78.8	77	0.3	6.8	7087	1.2	x
erythomycin	734	87.5	88	>10.0	8.3	364	−0.5	
indomethacin	358	68.5	69	>10.0	16.9	1382	0.8	
labetalol	328	95.6	66	>10.0	10.1	375	0.3	
loperamide	477	43.8	55	2.7	20.7	4820	1.8	x
nicardipine	480	119.8	69	0.0	8.8	81722	2.5	x
prednisone	358	91.7	73	4.9	4.8	209	−0.2	
propafenone	342	58.6	93	9.4	19.1	7897	0.7	
quinine	379	45.6	73	9.4	12.6	828	0.4	x

Table 1 (Continued)

compd	MW [g/mol]	PSA [Å^2]	A_S [Å^2]	cmc [mM]	$\Delta\pi$ [mN/m]	K_{AW} [M^{-1}]	log K_{memb}	Pgp
			Region of False Negatives					
doxycycline	445	181.6	148	>10.0	5.4	201	−2.8	
fluconazole	306	81.7	131	>10.0	3.6	176	−2.3	
fluphenazine	438	55.3	113	5.0	4.8	480	−1.2	x
probenecid	285	83.1	174	>10.0	6.0	888	−3.1	
testosterone	288	37.3	127	0.7	4.3	3067	−0.9	

[a] Compounds that did not reach the cmc or solubility limit are denoted by "maximum applied concentration".

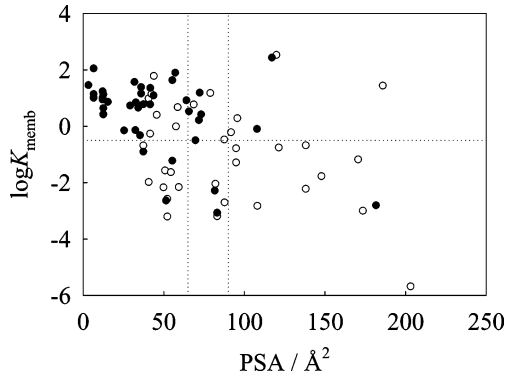

Figure 2. Correlation between log K_{memb} and polar surface area (● = CNS+; ○ = CNS−).

limit giving a good hit ratio for a smaller subset; e.g., for the set of compounds shown in this paper the 90 Å^2 limit results in only three false negatives above the 90 Å^2 limit. Nevertheless, neither value can distinguish between the two in vivo classes for the whole set. The membrane partitioning approach, log K_{memb} (the horizontal dotted line), although not performing distinctively better in overall predicitivity, nevertheless separates CNS and non-CNS compounds more clearly into two groups. The fundamental difference between PSA and log K_{memb} is that the latter describes experimental molecular properties in an anisotropic medium, while the fragment-based PSA disregards molecular conformations and accessibility because of steric factors and thus may also account for atoms that are not available for hydrogen bonding.

Drawbacks of the current approach for obtaining a high hit ratio are the lack of surface activity for a large number of compounds and the inclusion of both passively and actively transported compounds. Yet this method provides a straightforward, domain knowledge based assessment, which is both reasonable and physically justified. This is seldom the case for models founded on multivariate statistics, which can also be prone to overtraining. To avoid overfitted models, large high-quality data sets provided with a sufficiently small number of independent variables are required. In this study, we believe that the lack of a large data set is not a key issue because the model is based on biophysical arguments, thus avoiding the pitfalls of multivariate statistics.

3. Conclusions

We have demonstrated the feasibility of a novel high-throughput platform for physicochemical compound characterization by surface activity profiling, along with its first application, the prediction of passive uptake into the brain. A membrane partitioning coefficient, K_{memb}, was derived and successfully used to distinguish compounds capable of crossing the BBB. This parameter also identified those compounds, which due to their membrane activity are likely to be transported by Pgp. Unlike other methods of assessing membrane partitioning, surface activity profiling gives information projecting not only lipophilicity but also molecular size, flexibility, and orientation in the interface. On the basis of the obtained results for blood−brain barrier permeability prediction, we suggest that surface activity profiling provides a fast screening technique yielding parameters that relate more generally to interactions between compound structure and in vivo activity.

4. Experimental Section

Sample Preparation. The compounds were obtained from various manufacturers and were used as received without further purification. The minimum purity of the studied compounds was 95%. To this end the purity requirement of the assay is high because of the sensitivity of the method to any surface active contaminants. Default stock solutions were 100 mM of the respective compound in DMSO. A dilution series of 11 concentrations of each compound was prepared in DMSO with the concentrations given by 100×2^{-n} mM where n ranges from 10 to 0, obtained using a dilution ratio of 1:1. The serial dilutions were prepared in disposable 96-well plates with one compound per row with an in-house-built liquid handling workstation (Kibron Inc., Helsinki, Finland). The last column was filled with pure DMSO, providing a reference (γ^0; see below). Five microliters (5 μL) from each well in the dilution series was transferred onto small-volume 96-well measurement plates (detection plate), optimized for surface tension measurements. Subsequently, 45 μL of the measurement buffer (buffer A, Kibron Inc.) was added to each well. Accordingly, the maximum concentration on the measurement plate was 10 mM. The contents were thoroughly mixed, and the plate was allowed to stand under a lid for 10 min in order to achieve a sufficient degree of partitioning of the compounds between the bulk and surface.

Measurement Procedure. Surface tension measurements were carried out on a multichannel microtensiometer (Delta-8, Kibron Inc.). The instrument utilizes eight parallel microbalances fixed to meet the positions of the wells of the 96-well plate format. While the surface tension measurement is based on the Du Nouy method, our approach utilizes small needles (probes) instead of a Du Nouy ring. The probes have a diameter of 0.5 mm, and the measurement solutions are assumed to completely wet the surface of the probe. The maximum force exerted by the surface tension is recorded as the probes are withdrawn from the solution. The instrument features automatic cleaning of the probes by heating prior to the measurement of the 96-well plate. The plates are measured starting from the DMSO/buffer solution (to account for the effect of DMSO on surface tension) and then advancing in the order of increasing drug concentration to avoid carry-over. The entire measurement sequence requires less than 2 min, yielding a theoretical throughput of over 1500 compounds in an 8 h working day.

Analysis of the Adsorption Isotherm. Surface tension, γ, is defined as the work, dW, required to expand a surface by an area dA,

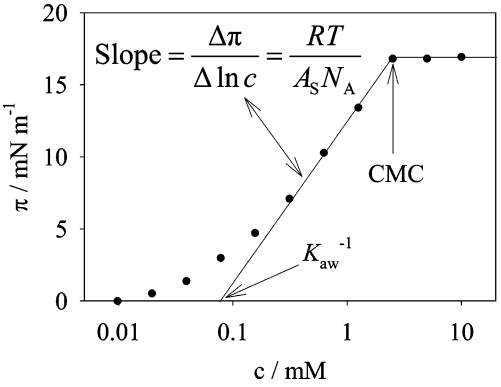

Figure 3. Characteristic parameters obtained from the adsorption isotherm: critical micelle concentration (cmc), air/water partitioning coefficient (K_{aw}), and molecular cross sectional area (A_S). This example shows the adsorption isotherm of verapamil.

$$\gamma = \frac{dW}{dA} \tag{1}$$

and results from an imbalance in intermolecular forces at the surface of a liquid. It is thus a direct measure of the energy needed to form a new surface of unit area. The defining characteristic of surfactants, in this case drugs that are studied, is their ability to lower surface (interfacial) tension by partitioning into the interface. In this study, we focus on the accumulation of a drug from the aqueous phase into the air/water interface. This phenomenon is well described by classical thermodynamics, more specifically, by the Gibbs adsorption isotherm, which relates the surface excess Γ to the chemical potential μ of the drug through

$$\Gamma = -\frac{1}{RT}\frac{d\gamma}{d\mu} \approx -\frac{1}{RT}\frac{d\gamma}{d\ln c} \tag{2}$$

where R is the gas constant, 8.314 J mol^{-1} K^{-1}, T is the temperature, and c is the concentration of the drug. The latter equality follows in the infinite dilution limit where $d\mu = d\ln c$. Commonly, an equation of state for the surface phase is used with the Gibbs adsorption isotherm in order to obtain a relationship between the bulk concentration and the surface tension. However, while the Gibbs isotherm follows from a thermodynamic derivation, equations of state require assumptions pertaining to the molecular interactions in the system. The drug molecules that are being considered are both complex and structurally diverse, and therefore, their behavior is difficult to describe by a single equation of state. Accordingly, only the Gibbs adsorption isotherm will be used in the analysis described below.

For convenience, we use surface pressure, which is related to surface tension through

$$\pi = \gamma^0 - \gamma \tag{3}$$

where γ^0 is the surface tension of the bare interface and γ is that in the presence of surface active substances. A typical surface pressure isotherm as a function of bulk concentration is shown in Figure 3.

For monolayers, the difference between surface concentration and surface excess becomes negligible. The surface concentration is inversely proportional to the area available per surfactant molecule in the interfacial region. Thus, the molecular cross-sectional area of one molecule is given by

$$A_S = \frac{1}{N_A \Gamma} \tag{4}$$

where N_A is Avogadro's number, 6.022×10^{23} mol^{-1}. This relationship is particularly useful at higher surface pressures where the surface concentration is limited by the molecular cross-sectional area; i.e., in this region the slope of the isotherm remains constant (Figure 3). This is commonly assigned to the hard disk area of the surfactant molecule.

The critical micelle concentration (cmc) or solubility limit results in a sharp transition above which the concentration of the free drug remains constant, resulting in a plateau in the surface pressure. Thus, the intersection of the two fitted lines determines the cmc or solubility (Figure 3). Currently, we cannot distinguish between the two phenomena.

Unfortunately, the Gibbs adsorption isotherm does not provide a direct means for an unambiguous determination of the standard air/water partitioning coefficient. Instead, we will use a parameter, i.e., an apparent partitioning coefficient, that to a satisfactory level quantifies the partitioning. In this study, the apparent partitioning coefficient, K_{aw}^{-1}, is determined as the intersection between the extrapolated line and log c (x-axis). It is inherently assumed here that the slope of π versus ln c is constant, i.e., the molecular cross-sectional area has reached a constant limiting value. Further, the apparent partitioning coefficient will be used as a standard state. The adsorption energy is then given by $\Delta\mu^0_{aw} = -RT \ln K_{aw}^{-1}$. The alternative and more common definitions of the standard state of an adsorbed monolayer are (i) half coverage in absence of molecular interactions or (*ii*) surface pressure increase of $\pi =$ 1.0 mN/m.[26] The former, in particular, is difficult to assess from experiments involving complex molecules, since it must be corrected for molecular interactions. However, the apparent partitioning coefficient used here is extrapolated from higher surface pressures and includes molecular interactions in the monolayer that are observed at the air/water interface. This is particularly useful in the estimation of a membrane partitioning coefficient discussed below.

Membrane Partitioning Coefficient. Although the air/water interface and the lipid/water interface of the bilayer differ in their structure, partitioning into both interfaces is mainly driven by the hydrophobic effect, arising from the reduced entropy due to organization of water around hydrophobic groups. The main difference between these interfaces is the equilibrium lateral pressure exerted in the lipid monolayer, which is used as a first approximation to obtain the membrane partitioning coefficient. This approximation is easy to implement with the standard state described above and does not require determination of higher order drug−lipid interaction coefficients. We start from the Butler equation,[26] which relates the chemical potential to the surface tension through

$$\mu = \mu^0 + RT\ln(f\chi) - \gamma A_S N_A \tag{5}$$

where μ and μ^0 are the chemical potential and the standard chemical potential, respectively, f is the activity coefficient, and χ is the molar fraction of a drug molecule in the membrane. We are interested in the quantitative change in the standard chemical potential when a molecule is transferred from the air/water interface into the hypothetical membrane leaflet. Thus,

$$\Delta\mu^0_{memb} = RT \ln K_{memb} = \Delta\mu_{ads} + (\gamma - \gamma^0_{memb})A_S N_A = RT \ln K_{ads} - \pi A_S N_A \tag{6}$$

where $f_i\chi_i$ has been assumed to remain constant. In the above, $\Delta\mu_{ads}$, γ^0_{memb}, and K_{ads} represent the chemical potential, surface tension, and the partition coefficient for the adsorption in to the membrane leaflet. Thus,

$$\log K_{memb} = \frac{RT\ln(K_{aw}) - \pi_{memb} A_S N_A}{2.302RT} \tag{7}$$

where K_{aw} is the air−water partition coefficient, A_S is the molar cross-sectional surface area of the drug at the air/water interface, and π_{memb} is the equilibrium lateral pressure of the bilayer membrane, 34 mN/m.[11] The above equation states that in order for a molecule to partition into the membrane, work must be done against the lateral pressure that prevails in the

membrane. Thus, partitioning is favored for compounds having high affinities for the air/water interface and small cross-sectional areas, while binding diminishes for compounds with small air−water partitioning coefficients and large surface areas. K_{memb} differs from other measures of lipophilicity as is also the cross-sectional area; i.e., effective molecular shape is taken into account. Furthermore, the air−water partitioning coefficient is inherently dependent on the spatial distribution of the polar and nonpolar moieties in the molecule.

References

(1) Lohmann, C.; Huwel, S.; Galla, H.-J. Predicting blood−brain barrier permeability of drugs: Evaluation of different in vitro assays. *J. Drug Targeting* **2002**, *10*, 263−276.

(2) Kansy, M.; Senner, F.; Gubernator, K. Physicochemical high throughput screening: Parallel artificial membrane permeation assay in the description of passive absorption processes. *J. Med. Chem.* **1998**, *41*, 1007−1010.

(3) Artursson, P.; Palm, K.; Luthman, K. Caco-2 monolayers in experimental and theoretical predictions of drug transport. *Adv. Drug Delivery Rev.* **2001**, *46*, 27−43.

(4) Di, L.; Kerns, E. H.; Fan, K.; McConnell, O. J.; Carter, G. T. High throughput artificial membrane permeability assay for blood−brain barrier. *Eur. J. Med. Chem.* **2003**, *38*, 223−232.

(5) van de Waterbeemd, H.; Kansy, M. Hydrogen-bonding capacity and brain penetration. *Chimia* **1992**, *46*, 299−303.

(6) van de Waterbeemd, H.; Camenisch, G.; Folkers, G.; Chretien, J.; Raevsky, O. Estimation of Blood−Brain Barrier Crossing of Drugs Using Molecular Size and Shape, and H-bonding Descriptors. *J. Drug Targeting* **1988**, *6*, 151−165.

(7) Lipinski, C.; Lombardo, F.; Dominy, B.; Feeney, P. J. Experimental and computational approaches to estimate solubility and permeability in drug discovery and development settings. *Adv. Drug Delivery Rev.* **1997**, *23*, 3−25.

(8) Testa, B.; Pliska, V.; van de Waterbeemd, H. *Lipophilicity in Drug Action and Toxicology*; VCH: Weinheim, Germany, 1995; Vol. 4, pp 22−24.

(9) Eytan, G.; Regev, R.; Oren, G.; Assaraf, Y. The Role of Passive Transbilayer Drug Movement in Multidrug Resistance and Its Modulation. *J. Biol. Chem.* **1996**, *271*, 12897−12902.

(10) Seelig, A.; Gottschlich, R.; Devant, R. M. A method to determine the ability of drugs to diffuse through the blood−brain barrier. *Proc. Natl. Acad. Sci. U.S.A.* **1994**, *91*, 68−72.

(11) Fischer, H.; Gottschlich, R.; Seelig, A. Blood−Brain Barrier Permeation: Molecular Parameters Governing Passive Diffusion. *J. Membr. Biol.* **1998**, *165*, 201−211.

(12) Fischer, H.; Seelig, A.; Chou, R. C.; van de Waterbeemd, J. The Difference between the Diffusion through the Blood−Brain Barrier and the Gastro-Intestinal Membrane. Presented at the 4th International Conference on Drug Absortpion, Edinburgh, Scotland, June 13−15, 1997.

(13) Seelig, A.; Landwojtowicz, E. Structure−activity relationship of P-glycoprotein substrates and modifiers. *Eur. J. Pharm. Sci.* **2000**, *12*, 31−40.

(14) Lullmann, H.; Lullmann-Rauch, R.; Wassermann, O. Lipidosis induced by amphiphilic cationic drugs. *Biochem. Pharmacol.* **1978**, *27*, 1103−1108.

(15) Casartelli, A.; Bonato, M.; Cristofori, P.; Crivellente, F.; Dal Negro, G.; Masotto, I.; Mutinelli, C.; Valko, K.; Bonfante, V. A cell-based approach for the early assessment of the phospholipidogenic potential in pharmaceutical research and drug development. *Cell Biol. Toxicol.* **2003**, *19*, 161−176.

(16) Yang, C.; Ansong, C.; Bockrath, L.; Chalmers, J. J.; Lee, Y.-S.; O'Neil, M.; Rathman, J. F.; Sakamoto, T. Mechanistic study of model monolayer membranes and their interactions with surfactants: correlation to effects on CHO cell cultures. *Stud. Surf. Sci. Catal.* **2001**, *132*, 435−438.

(17) van de Waterbeemd, H.; Camenisch, G.; Folkers, G.; Chretien, J. R.; Raevsky, O. A. Estimation of blood−brain barrier crossing of drugs using molecular size and shape and H-bonding descriptors. *J. Drug Targeting* **1998**, *6*, 151−165.

(18) Norinder, U.; Haeberlein, M. Computational approaches to the prediction of the blood−brain distribution. *Adv. Drug Delivery Rev.* **2002**, *54*, 291−313.

(19) Seelig, A. A general pattern for substrate recognition by P-glycoprotein. *Eur. J. Biochem.* **1998**, *251*, 252−261.

(20) Ertl, P.; Rohde, B.; Selzer, P. Fast Calculation of Molecular Polar Surface Area as a Sum of Fragment-Based Contributions and Its Application to the Prediction of Drug Transport Properties. *J. Med. Chem.* **2000**, *43*, 3714−3717.

(21) http://www-ra.informatik.uni-tuebingen.de/software/joelib/.

(22) van de Waterbeemd, H.; Mannhold, R. Programs and methods for calculation of log P-values. *Quant. Struct.−Act. Relat.* **1996**, *15*, 410−412.

(23) Lombardo, F.; Blake, J.; Curatolo, W. Computation of Brain−Blood Partitioning of Organic Solutes via Free Energy Calculations. *J. Med. Chem.* **1996**, *39*, 4750−4755.

(24) Schinkel, A. P-Glycoprotein, a gatekeeper in the blood-brain barrier. *Adv. Drug Delivery Rev.* **1999**, *36*, 179−194.

(25) Kelder, J. P. D. J.; Grootenhuis, D. M. Bayada, L. P. C. D.; Ploemen, J. P. Polar molecular surface as a dominating determinant for oral absorption and brain penetration of drugs. *Pharm. Res.* **1999**, *16*, 1514−1519.

(26) Aveyard, R.; Haydon, D. A. *An introduction to the Principles of Surface Chemistry*; Cambridge University Press: Cambridge, U.K., 1973; pp 79, 103−107.

JM0309001